JOURNAL OF PROPULSION AND POWER
Vol. 20, No. 2, March–April 2004

Parametric Design of Turbomachinery Airfoils Using Highly Differentiable Splines

Roque Corral*
Industria de TurboPropulsores, 28830 Madrid, Spain
and
Guillermo Pastor†
Universidad Politécnica de Madrid, 28040 Madrid, Spain

The primary purpose of this work was to develop a parametric tool to ease the generation of low-pressure-turbine airfoils. The present methodology was initially conceived to design turbine blades, and therefore some characteristics of the approach were oriented toward the solution of this specific problem; however, most of the basic formulation is readily extended to the design of other aerodynamic shapes (e.g., wings, compressors, etc.). The system combines a CAD-oriented methodology, where the user can interactively define the blade by means of control points, with the requirement of producing a highly differentiable curve. Both statements are essentially contradictory because high-degree polynomials tend to be extremely sensitive to variations in either their coefficients or control points and therefore not well suited for direct manipulation. The solution adopted is based on the generation of two chains of highly differentiable Bézier curves, where the design is carried out in the downstream direction. A methodology is described to generate low-pressure-turbine airfoils as well as other types of airfoils.

Nomenclature

a	=	major semi-axis of the leading-edge ellipse
b	=	minor semi-axis of the leading-edge ellipse
bsd	=	backsurface diffusion angle
$\boldsymbol{C}$	=	generic curve
C_p	=	pressure coefficient
c	=	axial chord
K	=	curvature
M	=	relative Mach number
n	=	intrinsic coordinate normal to the streamline
$\boldsymbol{n}$	=	normal vector to a curve
$\boldsymbol{P}$	=	control point
R	=	radius of curvature
$Re_{2,\mathrm{is}}$	=	isentropic exit Reynolds number
$r_{\mathrm{t.e.}}$	=	trailing-edge radius
r_{th}	=	throat radius
S	=	entropy
S_b	=	pitch
s	=	arc length; intrinsic coordinate along the streamline
Tu	=	turbulence level
u	=	curve parameter
$\boldsymbol{V}$	=	velocity vector
$w_{\mathrm{t.e.}}$	=	trailing-edge wedge angle
w_1	=	leading-edge suction side wedge angle
w_2	=	leading-edge pressure side wedge angle
α_1	=	inlet metal angle
α_2	=	outlet metal angle
λ	=	stagger angle
ρ	=	density

Received 31 March 2003; revision received 4 August 2003; accepted for publication 4 August 2003.

*Head, Technology and Methods Department; also Associate Professor, School of Aeronautics, Universidad Politécnica de Madrid, 28040 Madrid, Spain.

†Research Assistant, School of Aeronautics; currently Research Engineer, Industria de TurboPropulsores, 28830 Madrid, Spain.

Introduction

GAS-TURBINE blades are three-dimensional objects operating in a complex flowfield. This complexity has given rise to the decomposition of the analysis of the flow in the sum of a series of two-dimensional problems. Depending on the aspect ratio of the blade, this hypothesis is more or less close to the reality, but in any case the usual practice is to design each section as if this hypothesis holds. In a second stage the airfoils are stacked following design rules for the locus of a common point in the sections (e.g., the center of gravity or the trailing edge), and three-dimensional analyses are carried out to verify the aerodynamics and modal behaviour of each new geometry. The blade-design sequence varies among different engine manufacturers, but all of them follow essentially the same philosophy. Usually the two-dimensional design of the sections is carried out as a combination of direct and inverse methods, but still the involvement of the designer's insight in the process is essential.

Basically two different approaches are possible to parameterize a blade. The first one consists in defining the aerodynamic surface by means of a set of points that in principle can be placed in arbitrary positions. The number of nodes involved in such definition might be large, of the order of several tens, and thus the process of moving those points with the aim of achieving a target Mach-number distribution can be troublesome. The number of available degrees of freedom (DOF) is thus twice the number of points; however, constraints related with a certain degree of differentiability of this discretized curve have still to be imposed over that distribution. The final result is that one of the designer's task is, either manually or with the help of inverse design codes, to remove those spurious DOF and retain only the relevant ones. Discontinuities in the curvature distribution are prone to occur during this process, and the use of inverse methods is needed to help the designer in eliminating spikes in the Mach-number distribution. The main advantages of this technique are the lack of restrictions in the placement of the nodes and the easiness of communication with codes with the capacity to perform inverse design because their internal representation of the geometry is usually based on a cluster of points and therefore the communication takes place in a natural way.

The second approach defines the blade by a set of curves; the problem then is to find a suitable subset capable, not only to represent the desired shape, but easily amenable to the user manipulation. CAD curves are usually represented as rational polynomials (NURBS). In principle, other sets of functions could be chosen to define the

blade inside our system; however, it is expected that at some stage of the design the geometry will be transferred to a CAD system, and if the designed geometry might not be exactly represented there the potential danger of a loss of accuracy in its representation exists, because a fitting process will be required to translate the geometry from one system to the other. To avoid this uncertainty, we have chosen a set of basis functions that are fully compatible with all CAD systems. The main advantage of this type of approach is the ease of the designer's work, which allows him to work only with the physically relevant parameters as the major and minor radius of the leading edge (l.e.) the airfoil throat radius, etc., without paying attention to the degree of continuity of the final curve, that is guaranteed by a proper selection of the basis functions. One of the drawbacks of this method is that its combination with inverse design programs that internally use either a pointwise definition of the surface, a prescribed basis of functions, or a mixed of both,[1] requires an interface to translate blade parameters in terms of points to avoid retrieving the blade surface upon the direct modification of the blade points.

Early parametric design methods were based on the specification of the airfoil thickness around a camber line[2]; however, the different nature of the physical phenomena that take place in the suction and pressure sides of the airfoil has promoted the development of methods with independent control of each surface. More recently, Korakianitis[3] and Korakianitis and Papagiannidis[4] showed the importance of the airfoil curvature distribution in its performance and described a potential method to design highly differentiable blade surfaces.[3–5,6] Firstly,[3] he developed a parametric method based on a blending of third- and fifth-order polynomials of the form $y = f(x)$, plus an ad hoc treatment of the leading-edge geometry. This region was designed by specifying a thickness distribution that was added perpendicularly to two independent parabolic lines, one for the suction side and another for the pressure side, that passed through the nominal leading edge. The main disadvantage of the method was that the continuity of the derivative of the curvature had to be attained during the design of the blade and, unless special attention was paid to remove slope curvature discontinuities oscillations in the Mach-number distribution might appear. To circumvent this problem, a second method was proposed,[7] where the continuity in the slope of the curvature was achieved by means of a set of fourth-order splines of the form $x = x(u)$ and $y = y(u)$. They found this method expensive in terms of CPU time and abandoned the method in favour of a third one.[5] In this approach the blade was defined using three different representations. The leading-edge region used the definition described in the first method; the zone of unguided diffusion was represented by a third-order polynomial, and in the rest of the blade the curvature was directly specified by means of a Bézier polynomial. Still problems were reported by the author to find a proper curvature distribution for this segment.

All of the difficulties encountered in the previous works are associated to the high sensitivity of the geometry to small changes in the parameters because of the presence of high-order derivatives in its formulation. Small perturbations in the node positions (of the order of $10^{-4}c$) can give rise to modifications on the curvature perceptible in the Mach-number distribution. The difficulty of the problem and the lack of a built-in human intuition for its solution lies in its dependence on high-order derivatives and the existence in the blade of regions whose curvatures differ by orders of magnitude.

In this work we have developed a set of chained G^3 Bézier polynomials where the design is carried out in the downstream direction. The design tool based on that set of polynomials, named XBlade, posses a CAD-oriented methodology, and the user can interactively manipulate the control points of each segment in order to achieve the desired shape while the continuity of the slope of the curvature is preserved at any moment. To monitor the design process plots of the curvature, the channel width and the C_p, obtained by means of either an incompressible panel solution or an Euler code coupled with an integral boundary layer, are displayed in real time. Special attention is paid to control the instabilities originated by the high sensitivity of the problem to small modifications on the control points.

Blade Curvature: Flowfield Influence

To clarify what the design requirements of the blading system should be, a number of subjects must be addressed in advance. The issue of the manufacturability of the blades should be ideally taken into account at this stage; we will focus however on the aerodynamic point of view of the problem. A few comments about this problem can be found in Corral and Pastor.[8] The first question that needs to be answered is what is the minimum degree of continuity of the analytical representation of the blade. The aim of the aerodynamic designer consists of producing aerodynamic shapes that yield the desired load minimizing the losses and satisfying some mechanical restrictions. The intuition indicates that, if the flow remains attached to the wall surface, such a goal is fulfilled somehow when the aerodynamic surface is as smooth as possible. It is widely admitted that the presence of uncontrolled discontinuities in aerodynamic surfaces is undesirable because they increase the boundary-layer thickness and might potentially promote or inhibit its transition or separation[9]; therefore, it is common sense that aerodynamic profiles need to be at least C^1 (i.e., have their slope continuous). It is well known however that in complex flowfields sharp devices can improve the global aerodynamic performance inducing transition or reattachment of the flow by means of complex vortex interactions. This type of gadgets can be clearly seen in aircraft wings to improve the stall behavior (vortex generators) and in nacelles (fences) to remedy aerodynamic malfunctions caused by engine installation effects without conducting a new redesign. In the absence of these complications, the aerodynamic designer looks for smooth geometries. It must be stressed however that in certain cases transition is promoted on purpose to delay separation and reduce the total losses.

Theoretical Influence

The point then is: what is the minimum degree of continuity of a curve that ensures a smooth pressure distribution? An heuristic answer to this problem can be obtained by writing the momentum equation for an inviscid flow in the intrinsic frame of reference formed at each point by the tangent to the local streamline and its perpendicular:

$$v\frac{\partial v}{\partial s} = -\frac{1}{\rho}\frac{\partial p}{\partial s} \tag{1}$$

$$\frac{v^2}{R} = \frac{1}{\rho}\frac{\partial p}{\partial n} \tag{2}$$

Because the blade surface is a streamline, we can use Eqs. (1) and (2) to describe the flow in the vicinity of the blade. The main idea is to study the stream tube in contact with the surface of the blade and estimate the effect of the radius of curvature on the baseline pressure distribution. It must be kept in mind that the baseline solution depends on global parameters such as the inlet metal angle or the stagger angle, whereas the perturbations take into account only the local influence of the curvature in the flowfield. The basic assumption is that the stream-tube modification caused by curvature perturbations about its baseline value is small. In other words, the main hypothesis is that the blade modifications we are considering are so small that their influence on the passage area of the blade is negligible. This is usually the case in the final stages of the aerodynamic design when small modifications of the blade are made in order to achieve a target Mach-number distribution. During this phase, the modifications of the blade are tiny; however, significant modifications on the Mach-number distribution are still obtained. This behavior can only be explained by local effects associated to curvature perturbations because the overall definition of the blade geometry remains essentially the same.

Assuming that the perturbations of the flowfield about the baseline configuration have constant total pressure and total temperature that are constant, it is possible to derive a closed form for the perturbations of any of the independent variables (see Ref. 8). The

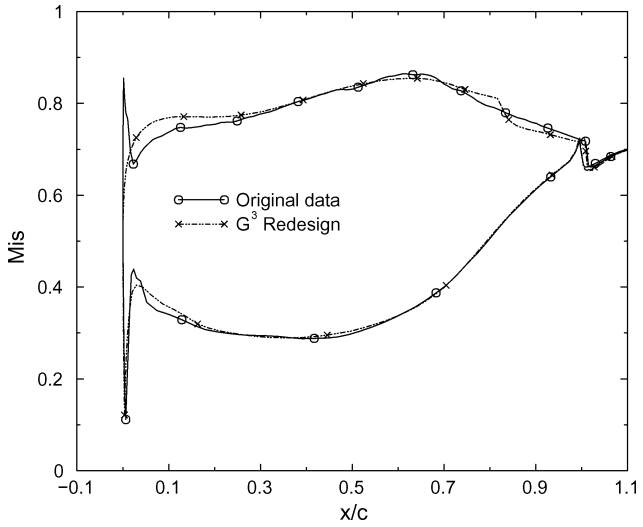

Fig. 1 Mach-number distribution of a blade profile defined as the blending of a l.e. circle and a cluster of points[10] and a redesign of it.

first-order term of the perturbed equation is of the form:

$$\bar{v}\frac{\partial \bar{v}}{\partial s} + \frac{1}{\bar{\rho}}\frac{\partial \bar{p}}{\partial s} = \frac{\bar{v}^2}{R}\frac{n}{R}\frac{\partial R}{\partial s} + (h.o.t.) \tag{3}$$

where the bars refer to the baseline values of the variables. The preceding expression highlights the influence of the curvature on the pressure distribution.

Experimental and Computational Evidences

Experimental evidence of the effect of curvature discontinuities on the pressure distribution is difficult to find mainly because of the lack of enough measurement resolution in the region of interest. However, Hodson[10] experimentally detected the presence of a leading-edge spike as a result of a curvature discontinuity in the blending point between the circle that defines the leading edge and the rest of the blade. He admitted that the detection of this spike was fortuitous because it was not possible to detect it in all of the cases, even for the same operating conditions. Computational experiments confirm the existence of this overspeed region (Fig. 1). It can be clearly seen how the spike in the Mach-number distribution is caused by the l.e. curvature discontinuity and is eliminated in a redesigned continuity in the slope of the curvature. Experimental works[9] have acknowledged the need to take into account the leading-edge wedge angle to account for leading-edge losses at off-design conditions. Curvature discontinuities at the leading edge have a more severe impact in performances at off-design conditions because at least one of the discontinuities takes place in a region of high velocity. In case of positive incidence, the discontinuity of the suction side is in a region of higher velocity than the one of the pressure side, whereas if the incidence is negative the same will be true for the pressure side. Benner et al.[9] concluded that the leading-edge wedge angle must be maximized in order to reduce the penalty in performance caused by the blending point discontinuity. This conclusion is implicit in Eq. (3).

The effect of discontinuities in the slope of the curvature in the suction side of a turbine blade has been studied by Koriakinitis.[5] They made some computational experiments and showed that the curvature and the Mach-number distribution behaved qualitatively in the same way and that discontinuities in the slope of the curvature were directly translated into the Mach-number distribution. Their simulations and ours are consistent with Eq. (3) as well.

Discontinuities in the slope of the curvature can be detected as well in the leading edge; however, because of the existence in this area of high-Mach-number gradients and usually less grid resolution they are harder to see. Koriakinitis[6] displays a case where one of such discontinuities can be found in the l.e. region.

The conclusion from the preceding discussion is that it is necessary to keep at least continuity of the slope of the curvature on the blade surface to ensure that $\partial p/\partial s$ is continuous and avoid undesired anomalies in the Mach-number distribution over the blade.

Blade Parameters

The blade design sequence depends on global constraints of the component that typically impose: the velocity triangles at the inlet and outlet of the blade, or the gas angles, the number of blades, or the blade spacing, and their axial chord. All together fix the incompressible limit of the lift coefficient. The surface diffusion in the unguided part of the blade is controlled by the amount of turning after the throat. The proper value for each individual blade is based on empirical correlations, but the designer still has some freedom in its choice. The inclination of the blades with respect to the axial direction, the stagger angle, is a major choice for the designer and controls the overall shape of the blade. The trailing-edge thickness is determined by manufacturing constraints and is usually fixed during the design process. The throat area is an important parameter over which the designer tries to keep some control as well. If the blade is choked, the throat controls the mass flow; otherwise, the throat radius determines the maximum Mach number on the blade. Finally the leading and trailing edges are defined by their wedge angles, w_1, w_2, and w_e, and their local radii of curvature, a, b, and r_{te}. These parameters are intended to control the flow in the leading-edge region and are defined during the design sequence.

Once all of the preceding parameters have been set, it is possible to obtain the position and the slope of the limiting nodes of the leading edge with the body of the blade and the position of the geometric throat and the trailing edge (see Fig. 2). All of these data are derived just from the information contained in the 12 aforementioned parameters sketched in Fig. 3. The chord is just a reference length that is only needed to scale the geometry and set the Reynolds number.

CAD Curves

Background

Once the position and the slope of a certain amount of nodes have been fixed from the basic information provided by the designer, it would be desirable to build a set of polynomials that not only satisfy the aforementioned conditions, but that automatically ensure that the resulting curve is three times differentiable with respect to the arc length (i.e., is a curve of class G^3). Usually the designer is not interested in knowing the precise values of the curvature and its derivatives, and therefore it is expected that this information be provided as a byproduct of any method. Several approaches are possible to obtain a polynomial representation of a curve that fits a number of points (see Ref. 11 for a review of different methods as well as for a review of CAD curves). The first decision that has to be taken is whether a global representation (i.e., a unique function extending across the whole domain is used to represent the geometry) or a local approximation (i.e., a set of interconnected curves) is desired. Global approximations of complex shapes require a prohibitively high degree of the approximating polynomial in order to accommodate all of the details of the geometry and are not well suited to interactive design. Therefore, most of the methods fall in the second category and are based on piecewise polynomial curves (i.e., splines). Polynomials can be expressed in different forms, among

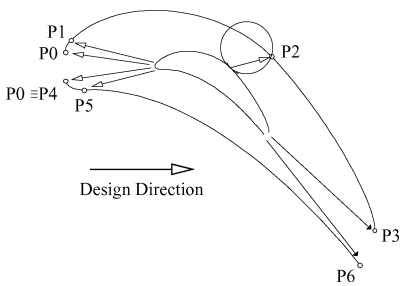

Fig. 2 Sketch of the Bézier chains used in the definition of the airfoil.

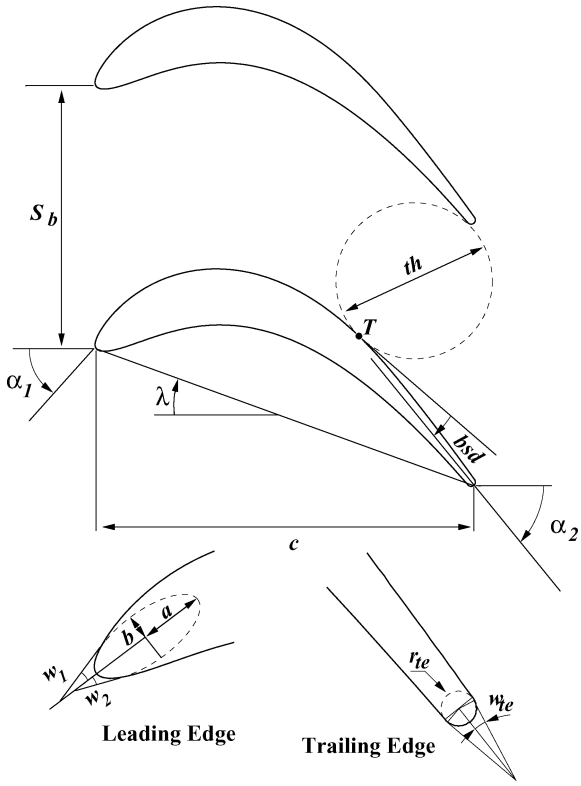

Fig. 3 Basic parametric definition of the blade.

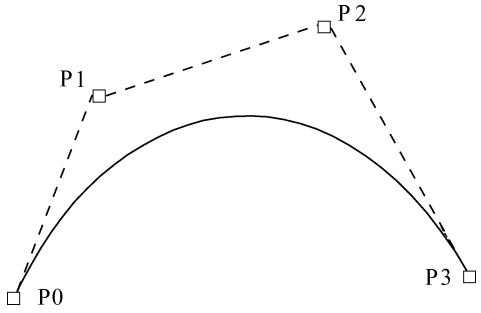

Fig. 4 Control points of a third-order Bézier polynomial.

them, and from the point of view of the end user; one of the more interesting ones is the so-called Bézier form. A Bézier curve is obtained as a linear combination Bernstein polynomials:

$$B_{i,n}(u) = \frac{n!}{i!(n-1)!} u^i (1-u)^{n-i} \tag{4}$$

of the form:

$$\boldsymbol{C}(u) = \sum_{i=0}^{n} B_{i,n}(u) \boldsymbol{P}_i \tag{5}$$

Their most interesting feature is that the so-called control points $\boldsymbol{P}_i$ are directly related with the values of the derivatives at the endpoints of the curve (see Fig. 4). $\boldsymbol{P}_0$ and $\boldsymbol{P}_1$ control the slope at $\boldsymbol{P}_0$ and $\boldsymbol{P}_0$; $\boldsymbol{P}_1$ and $\boldsymbol{P}_2$ fix the value of the second derivative at $\boldsymbol{P}_0$. When used in a CAD system, $\boldsymbol{P}_1$ and $\boldsymbol{P}_2$ are used to control the shape of the curve to match a prescribed geometry but not to assign the second derivative (or the curvature) to the endpoints.

The Hermite form of a polynomial relates in a direct manner the polynomial coefficients with the values of its derivatives at the endpoints:

$$\boldsymbol{C}(u) = \sum_{i=0}^{m} H_{i,n}(u) \boldsymbol{C}^{(i)}(0) + H_{m+1+i,n}(u) \boldsymbol{C}^{(i)}(1) \tag{6}$$

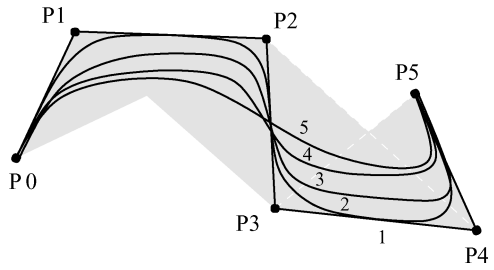

Fig. 5 B-spline with five control points.

Equation (6) sketches the Hermite representation of a polynomial of degree n [n is assumed to be even and $m = (n-1)/2$] defined by the values of its derivatives at the endpoints $\boldsymbol{C}^{(i)}(0)$ and $\boldsymbol{C}^{(i)}(1)$. However this representation is of limited help to the designer because, apart from the position and slope at the endpoints, this has a limited intuition about the influence on the geometry of the higher-order derivatives.

A pth-degree B-spline curve is a quite generic form of defining a piecewise polynomial curve and can be expressed as

$$\boldsymbol{C}(u) = \sum_{i=0}^{n} N_{i,n}(u) \boldsymbol{P}_i \qquad 0 \le u \le 1 \tag{7}$$

where $\boldsymbol{P}_i$ are the control points and $N_{i,p}(u)$ are the pth-degree B-spline basis functions that can be defined with the following recurrence formula:

$$N_{i,0}(u) \tag{8}$$

It is important to remark that the B-spline basis functions extend across different knots. This means that the lower the degree the fewer the control points that are contributing to the computation of $\boldsymbol{C}(u_0)$ for any given u_0 and the closer the B-spline curve follows its control polygon. The extreme case is $p = 1$, for which every point is a just linear interpolation between two control points (Fig. 5). Two properties are worth noting as well:

1) If $n = p$, then $\boldsymbol{C}(u)$ is a Bézier curve.

2) $\boldsymbol{C}(u)$ is infinitely differentiable in the interior of the knots intervals and is at least $p - k$ times continuously differentiable at a knot of multiplicity k.

Figure 5 depicts a B-spline with five control points. The numbers indicate the order of the spline. The first-order B-spline matches the control polygon, the second order is tangent to the control polygon, etc. The shaded area highlights the zone of existence of the polynomials according with the convex hull property.

At this point we can make a brief summary of the status of the problem. On the first hand, we have acknowledged the need of a basis of curves of class at least G^3 in order to satisfy a very stringent requirement on the differentiability of the resulting curve; on the second hand, we have found a family of curves, the B-splines, that could in principle satisfy this requisite, but that has little control to the precise location of inner points. A subset of the B-spline family, the Bézier curves, has been found to be optimal from the point of view of geometric modeling but lacks of enough flexibility to handle complex shapes. The concept of Bézier is related with a single polynomial and therefore might not deal with arbitrary geometries. Several Bézier polynomials can be easily put together to form a curve of class G^1, but its extension to curves with a higher degree of continuity is not straightforward.

Chained G^3 Bézier Curves

To overcome the aforementioned limitations, the formulation of a set of fourth-order G^3 chained Bézier curves was developed and implemented in an application known as XBlade. It was decided that each piece of the spline had to be, at least, fourth order to achieve a G^3 continuity at each breakpoint and still leave two degrees of freedom to the designer to accommodate the desired geometry. We

need to specify the coordinates and the slope of the curve at the beginning and the end of each segment (six restrictions). Furthermore, we need to impose

$$K^- = K^+ \tag{9}$$

$$\left.\frac{\mathrm{d}K}{\mathrm{d}s}\right|^- = \left.\frac{\mathrm{d}K}{\mathrm{d}s}\right|^+ \tag{10}$$

at each of the breakpoints, where the $-$ and $+$ superindexes denote the values at the left and right of the blending point; this means two conditions per segment in a cyclic spline. We have then a total of eight restrictions plus two design DOF per segment. Therefore, we need at least a fourth-order polynomial piecewise curve. This problem involves in practice the solution in real time of a complex set of nonlinear equations because

$$K(u) = \frac{\boldsymbol{C}''(u)\cdot\boldsymbol{n}}{|\boldsymbol{C}'(u)|^2} \tag{11}$$

and

$$K'(u) = \frac{\mathrm{d}K}{\mathrm{d}s} = \frac{\boldsymbol{C}'''(u)}{|\boldsymbol{C}'(u)|^3}\cdot\boldsymbol{n} - 3\left(\frac{\boldsymbol{C}''(u)\cdot\boldsymbol{n}}{|\boldsymbol{C}'(u)|^2}\right)\left(\frac{\boldsymbol{C}''(u)\cdot\boldsymbol{t}}{|\boldsymbol{C}'(u)|^2}\right) \tag{12}$$

To circumvent the problem of the solution of a global system of nonlinear equations where all of the segments are interrelated, we have made some simplifying hypothesis that ease its solution and at the same time are convenient for this specific problem. We have assumed that at one of the end points of the spline K and K' are known. This is the case at the nominal stagnation point of airfoil at its design condition where K' vanishes because of the local symmetry and K is the inverse of the radius of curvature at the l.e. The latter is a natural condition at the stagnation point because it has a strong influence in the off-design behavior and the global shape of the blade. We can then anticipate that we are using two chains of Bézier curves, one for the airfoil suction side (s.s.) and one for the airfoil pressure side (p.s.), both of them are supposed to begin at the stagnation point of the design condition.

Once the position and slope of the first and last control points of the first segment $\boldsymbol{Q}_0$ and $\boldsymbol{Q}_4$ (see Fig. 6) are chosen to satisfy the standard design parameters (wedges angles, t.e. thickness, stagger angle, etc.) and K_0 and K_0' are selected, the designer can move $\boldsymbol{Q}_1$ and $\boldsymbol{Q}_3$ along the prescribed tangents at the endpoints to make fine tuning of the blade with the two remaining DOF. The position of the control point $\boldsymbol{Q}_2$ is automatically derived for the designer from the prescribed data because already 10 constraints have been imposed for this curve. It is important to remark that the rest of the successive segments do not play any role in the determination of the position of $\boldsymbol{Q}_2$. At this instant K_4 and K_4' are known, and the same process can be repeated with the second segment. Hence there exists a design direction in the sense that any modification in one segment does not affect the curves located upstream in the same way that the local properties of a boundary layer are weakly influenced by anything that takes place downstream of that point. The designer then begins setting a proper configuration in the l.e. region and then proceeds downstream. During the process of adjusting the last segment of the suction side in order to tune the pressure gradient in the unguided part of the blade, all of the preceding segments are not influenced by this manipulation: what is an interesting property from the point of view of the designer. When it is detected that the desired behavior of the pressure distribution cannot be attained, this usually means that the designer has to come back upstream to fix first the previous curve. The design of a blade starting from scratch (i.e., an arbitrary initial shape) can be troublesome because all of the segments are affected by the modifications of the first one. This is not a problem in practice because the largest part of the aerodynamic designer work at this stage consists of redesigning departing from an earlier iteration. However, to alleviate this problem when no other data are around, a catalog of blades is provided with the program to help the designer in the initial stages of the design.

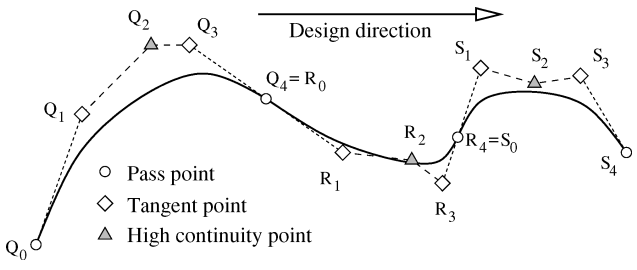

Fig. 6 Fourth-order G^3-chained Bézier curves. Each segment is defined by five control points.

A similar approach was attempted by Korakianitis and Pantazopoulos.[7] They developed a blading system based in fourth-order polynomials. However, in our opinion their method overspecified the number of restrictions at the blend points because instead of using Eqs. (9) and (10) they imposed

$$\boldsymbol{C}''(u)^- = \boldsymbol{C}''(u)^+ \tag{13}$$

$$\boldsymbol{C}'''(u)^- = \boldsymbol{C}'''(u)^+ \tag{14}$$

These are two more conditions than needed, because matching the derivatives of two functions with respect to an arbitrary parameter is somehow artificial in the sense that the intrinsic properties of the curve (e.g., the arc length, the curvature, etc.) are not involved; and in fact a reparameterization of the curve can produce a different spline. As a result of the overspecification of the boundary conditions in the breakpoints, two DOF per segment are lost, and therefore the number of curves required to specify a certain geometry had to be increased in their work. Koriakinitis[5] himself judged this method with criticism, mainly in terms of CPU time, and developed a new one. We believe that our method is faster because we do not have to iterate a coupled system of nonlinear equations for all of the curves because our method works in a segment-by-segment basis.

Geometric Blade Definition

The blade is represented by means of two chains of G^3 Bézier splines that are supposed to begin at the stagnation point for the design condition (see Fig. 2). The suction side is always represented by three curves, whereas the pressure side can be alternatively defined by just two to minimize the designer's number of DOF. Our experience is that in many cases two segments for the pressure side are enough to adjust the desired pressure distribution. However when the blades are very thin it is necessary to have the same number of curves at both sides to produce two quasi-parallel surfaces. The position and the tangent to the blade of all of the break points are inferred from the 12 basic parameters that define the blade. Besides the designer has two DOF per segment to fine tune the blade.

The first Bézier curve of each side is used to define the l.e. geometry. Because the blade shape is very sensitive to the modification of the l.e. control points, these are preset for the designer to increase the robustness of the method. Thus, the only DOF left at the l.e. are the major and minor axes and the wedge angles of the ellipse that are supposed to match the l.e. and that are mimicked by the Bézier curves. The point $\boldsymbol{P}_2$ (see Fig. 2) is special because it is forced to be at the throat of the blade and hence is over a circle of prescribed radius r_{th} that is tangent to the point $\boldsymbol{S}_0$ of the s.s. and the knot $\boldsymbol{S}_4$ of the adjacent blade pressure side (see Fig. 6).

Design Tool

The described chains of G^3 Bézier curves are integrated in a GUI, where the designer can interactively modify the blade shape changing both the global geometric parameters and the control points. To ease the understanding of the modifications and to guide the design in the right direction, not only the blade shape is displayed in real time but the curvature distribution, the channel and blade thickness, and an Euler solution coupled with an integral boundary layer. In

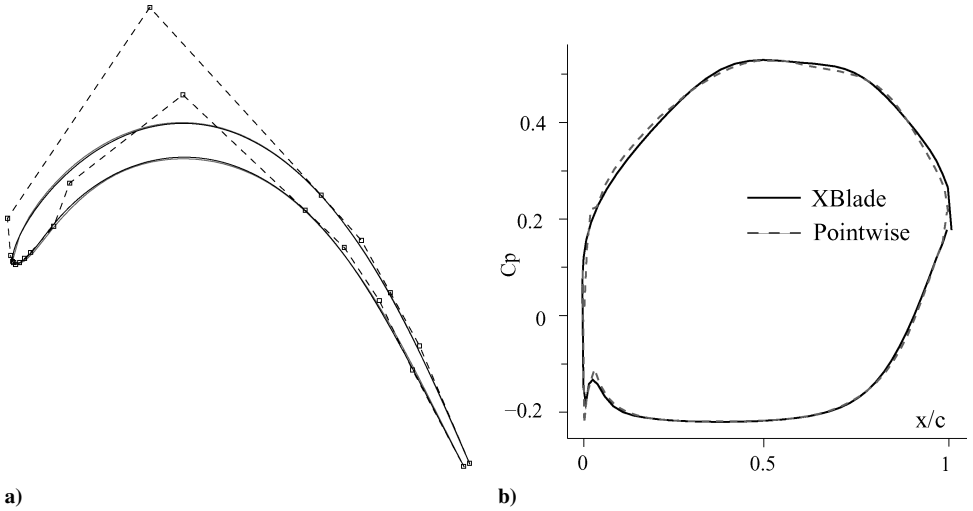

Fig. 7 Comparison of the a) geometry and b) incompressible pressure coefficient of a LPT airfoil designed using a pointwise method and the present parametric method.

this way not only the expected pressure distribution is automatically obtained but the position of the stagnation point at the design condition that is an important result for the designer. The use of inverse design programs at this phase of the design is not required because the pressure distribution obtained by this method is smooth and the elimination of spikes is not needed. At this stage the design is usually close to the final one, and just some minor modifications need to be done.

The capacity to monitor in real time black the isentropic Mach-number distribution of the blade has proved to be an invaluable tool for the designer to control the Mach-number distribution of the airfoil.

With the aim of dealing with the design of outlet guide vanes (OGVs), it is convenient to change the throat condition for this particular case. The underlying reason is that OGVs behave as compressor blades, have negative stagger angles, and the throat is located at the front of the blade. In this case the specified throat circle is tangent to the $\boldsymbol{S}_0$ point of the s.s. and the line that passes through the point $\boldsymbol{Q}_0$ of the next blade with a specified slope α_1. Thus, that circle is not actually the throat but a good approximation that discards the details of the leading-edge geometry. This parameterization depends weakly on the l.e. parameters a, b, $w1$, and $w2$, which might vary during the first steps of the design, providing a more stable suction side because $\boldsymbol{S}_0$ is not changed. This condition has proved to be quite useful in the design of this type of components.

It can be argued that because this approach has in principle fewer DOF than the pointwise approximation the designer remains all of the time inside a more limited universe and therefore can miss a more optimal solution. We believe that this is not true unless we face a completely new aerodynamic concept that could not be represented within the present approximation. This could be the case if we introduced grooved surfaces, fins, or any other new idea in the aerodynamic design that would include explicitly a discontinuity. Otherwise, our experience is that we have been able to reproduce all of the existent low-pressure turbine (LPT) and high-pressure turbine (HPT) pointwise designed airfoils that we have tried with enough fidelity. This is possible because in practice there are less than two DOF per node in the pointwise definition of the blade. If we tried to solve numerically the problem of designing a blade imposing that the slope, the curvature, and the slope of the curvature are continuous at each point, we would have more than three constraints per point, whereas the number of DOF is only two per knot. This means that in practice these conditions are not imposed at each node but only in a few of them. In other words there are less "true" DOF than the user believes. In fact, if we design a blade in a pointwise manner and we plot the curvature, there exist discontinuities on it. Actually, the distribution can only be considered continuous if we think in the blade as a mean, clean shape plus some roughness originated during the design process.

Figure 7 shows the degree of approximation that can be obtained designing with the current parametric method and a pointwise method with the help of an inverse design code. The geometry was designed during the standard design loop of a real engine and can be considered as a final airfoil. The geometry was traced afterward with the current method to demonstrate its capability to reproduce a representative airfoil. It can be appreciated that the degree of matching between both airfoils is very high (see Fig. 7a), actually the differences between them can be hardly appreciated even in scales five times larger than the one of the plot. The differences in the incompressible panel distribution (Fig. 7b) are not much larger either. The main idea is that in spite of both airfoils being designed independently by different designers using different approaches the final result is very similar. This demonstrates that the number of DOF of the current method is large enough to accommodate existing designs.

Figure 8 displays the curvature distribution for the same airfoil. The curvature was evaluated numerically in both cases departing from the files used by the solver to generate the mesh. This explains the small wiggles that are seen in the present method in the l.e. region that do not appear in the analytical evaluation of the curvature. It can be seen that the pointwise approach is much noisier in terms of curvature than the parametric method. On the right-hand side of the same figure, the circle representation used in the l.e. by the pointwise approach can be appreciated. The region of constant curvature (contaminated by some noise because of the discrete evaluation of the curvature) followed by a discontinuity can be clearly seen.

Application Examples

Up to now we have designed with the present method the two-dimensional sections of three LPTs including their OGVs. We have been able as well to reproduce a large number of designs made independently in a pointwise basis. Several HPT airfoils have been traced also to demonstrate the flexibility of the method. With the aim of giving an impression of the ability of the method to reproduce existing airfoils, we have traced several well-known airfoils available in the open literature.

A LPT airfoil[12] originally designed with a pointwise approach plus a circle representation for the l.e. has been traced. The original and the redesigned airfoils are shown in Fig. 9. The leading edge has been locally modified trying to keep the rest of the blade unaltered. The definition of the l.e. circle of the original blade can be easily distinguished. In this case it is specially difficult to match the original geometry because of the strong l.e. discontinuity in the airfoil, which is not explicitly taken into account in our method. The isentropic Mach-number distributions computed with MISES[1] for $M_{2,\mathrm{is}} = 0.71$, $Re_{2,\mathrm{is}} = 2.9 \times 10^5$, and $Tu = 0.5\%$ are shown in Fig. 1. The elimination of the l.e. spike in the Mach-number distribution

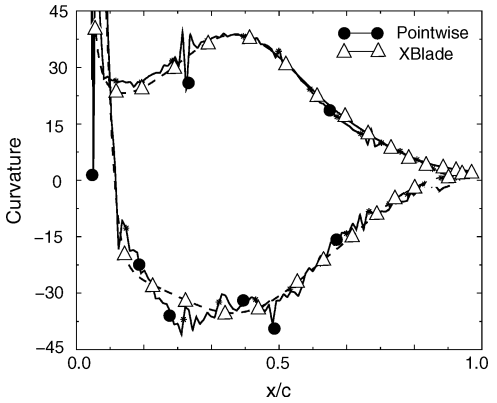

Fig. 8a Comparison of the curvature distribution obtained with a pointwise method (○) and the current method (△).

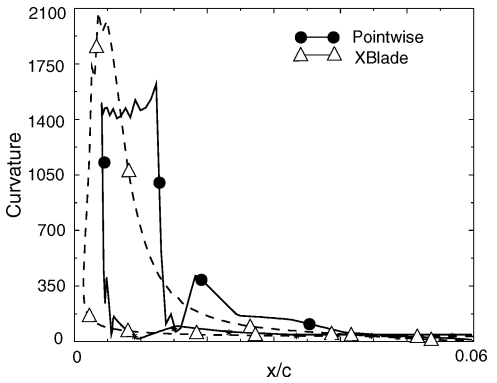

Fig. 8b Detail of the leading-edge region.

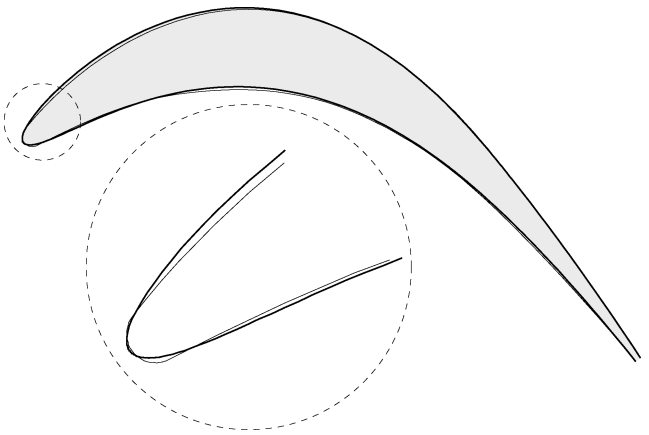

Fig. 9 Comparison of the blade profile of Hodson and Dominy[11] to a similar profile with a modified leading-edge geometry.

in the redesigned obtained with the parametric method is clearly appreciated. This spike is observed also in the experiments; but on the contrary in the simulations where the discontinuity is able to trip transition and the boundary layer is turbulent in the whole suction side, the flow remains laminar until 80% of the suction side where it separates and transitions. This is the behavior observed in the simulation of the redesigned geometry. The difference in losses between both cases is about 30%. The reason for the discrepancy between the losses computed for the original airfoil and the experiments is the lack of a built-in relaminarization mechanism in the method. In this particular case the l.e. spike, although undesirable because tend to promote transition, reduces to a computing inconvenience because the acceleration relaminarizes the flow. It is easy however to think in other situations with adverse pressure gradients where this would not be the case.

A typical curvature distribution obtained with this method is shown in Fig. 10. It is important to highlight the smooth transition

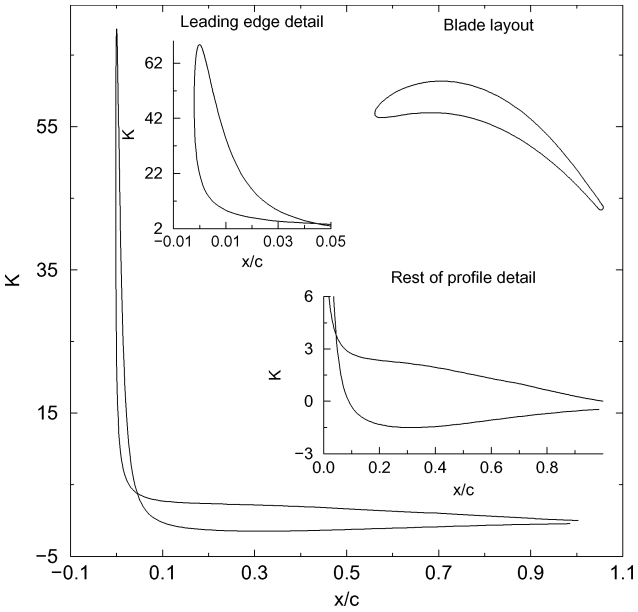

Fig. 10 Typical curvature distribution obtained with the present method. The high curvature of the blade in the l.e. region can be clearly distinguished.

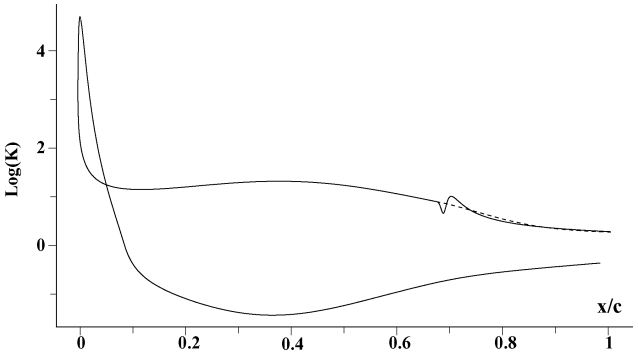

Fig. 11 Curvature distribution of a smooth blade (– – –), and an irregular blade (——) with a discontinuity on the curvature of its suction side created on purpose to trip transition.

from the l.e. region, with a very high curvature, to the nearly flat areas of the suction side. This behavior might not be obtained when circles are employed in the definition of the l.e. geometry and is characteristic of the present method.

Sometimes the designer is interested in tripping transition by means of a small discontinuity. This feature can also be achieved with this method because, although the curves are built with the aim of keeping the slope of the curvature continuous, the curve in practice can behave as if it were discontinuous if there exists a region where K' is very high. In practice the concept of continuity is related with the characteristic length of the problem. We can produce G^3 curves that in practice behave as discontinuous when they are regarded in a scale of the order of the chord length. Figure 11 depicts the curvature of two nearly identical blades. In one of them a "discontinuity" in the curvature has been created to trip transition. It can be observed that this discontinuity is local and does not alter the rest of the blade; in fact, both sections, not shown, cannot be distinguished by the eye.

The effect on the Mach-number distribution of discontinuities on the slope of the curvature has been previously investigated by Koriakianitis and Papagianidis.[4] To asses their conclusions, a special effort has been done to relax the degree of continuity of our system. The test has been done with an OGV section, where a discontinuity has been forced at the 30% of the axial chord. The curvature distributions of both blades are depicted in Fig. 12. We have tried to match both geometries in the discontinuity region; it is clear however that is not possible to match the rest of the blade

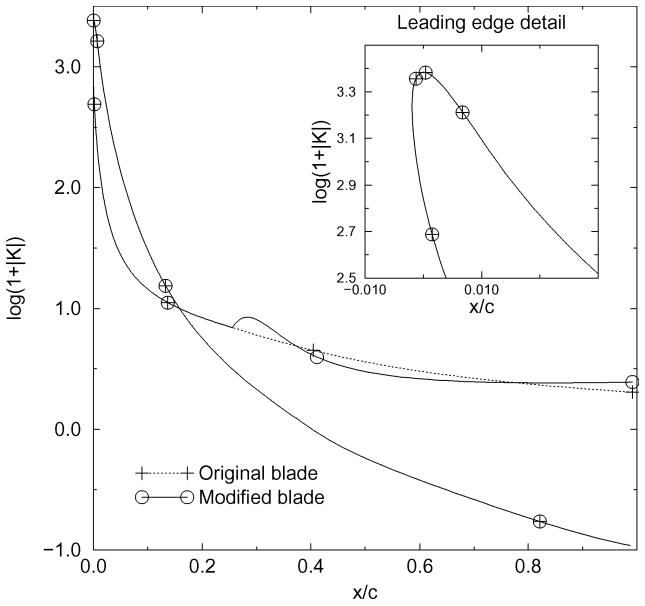

Fig. 12 Comparison of the curvature distribution of the blades of Fig. 13.

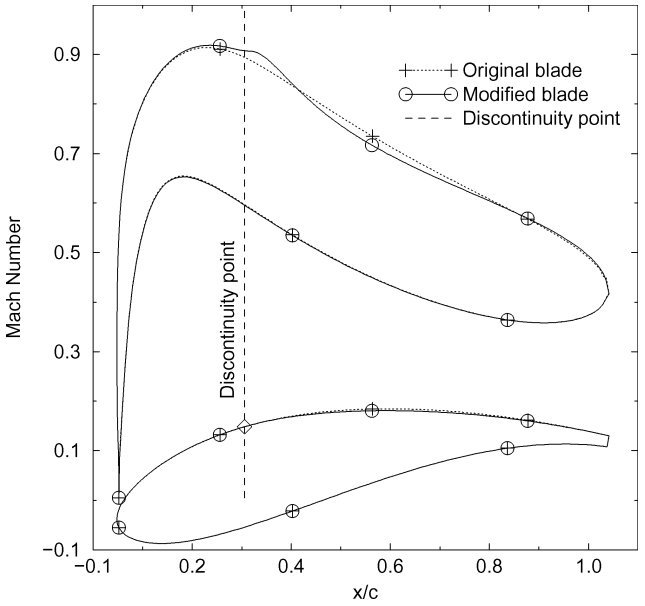

Fig. 13 Comparison of the Mach-number distribution of two different OGVs. In one of them a discontinuity in the slope of the curvature has been forced on purpose.

with the present constraints. In spite of the fact that both airfoils can be hardly distinguished (see Fig. 13), a bump in the inviscid Mach-number distribution, obtained with the MISES code,[1] is clearly seen in the discontinuity region. The conclusion is that discontinuities in the slope of the curvature are detected in the solution as it was expected. Although this case is highly transonic, the perturbations in the s.s. are confined to the discontinuity region and are not detected in the p.s. confirming as well the hypotheses that curvature perturbations are local in nature. The pitch-to-chord ratio of the OGV is 1.2.

To demonstrate the flexibility of the method, a highly loaded compressor corresponding to the 10th standard aeroelastic configuration[13] has been traced with the present method. Figure 14 displays the geometry and a detail of the l.e.; the original and traced geometry can be hardly distinguished, even in the l.e. close-up. The inviscid Mach-number distributions of both airfoils are seen in Fig. 15, where it can be appreciated that the differences between both distributions are obviously negligible from an engineering point of view.

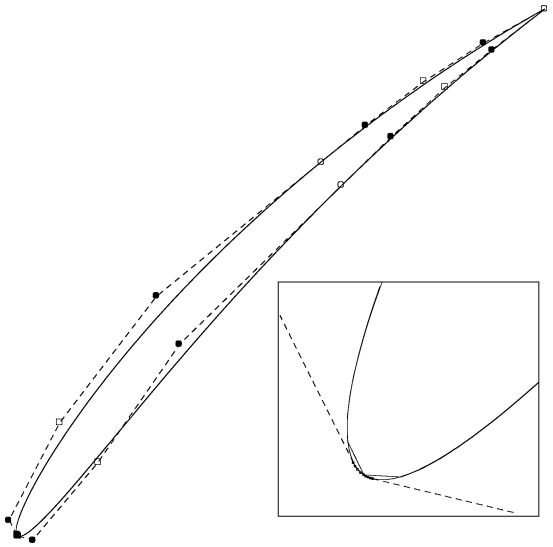

Fig. 14 Comparison of the original NACA 0006 compressor and the fitting with the present method.

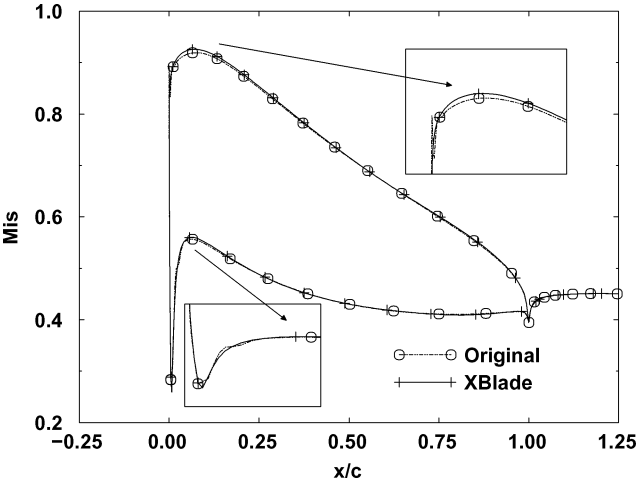

Fig. 15 Comparison of the Mach-number distributions of the NACA 0006 compressor and the fitting with the present method.

HPT blades can also be designed using the current procedure although this has not been specially customized for this purpose. Figure 16a shows a reproduction of the the LS89 cascade.[14] Both geometries, the original and the designed with the present method, can be hardly distinguished, and the corresponding Mach-number distributions for $M_{2,\mathrm{is}} = 0.7$ and $Re_{2,\mathrm{is}} = 10^6$ (Fig. 16b) are very similar. However the losses predicted by MISES[1] of the traced blade are about 12% lower than the ones of the original case because transition is delayed about a 10% of the axial chord, as a result of the increased smoothness of the blade surface. The transition point in the experiments[14] is located farther downstream, between 50–80% of the axial chord, depending on the freestream turbulence level. The main conclusion is that the transition point is very sensible to the freestream turbulence level and hence it can be reasonably expected that it will be similar to small imperfections in the blade that can promote transition. This behavior is seen in the numerical simulations and deserves special attention.

Figure 17 shows the flexibility of the method to design two nearly identical airfoils from an aerodynamic point of view with a quite different shape of the p.s. The first of them is very thin with a large bubble in the p.s., whereas in the second this bubble has been removed, thickening the blade trying to match the edge of the bubble with the airfoil. In the latter case a hollow blade will be manufactured leading to two quite different options from a mechanical point of view.

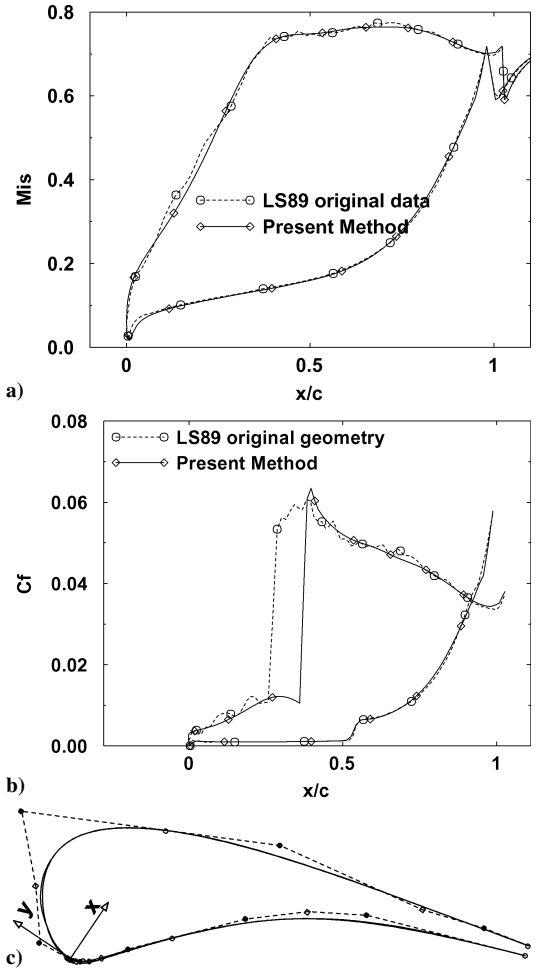

Fig. 16 Comparison of the a) isentropic Mach-number distribution, b) friction coefficient, and c) geometry of the original LS89 airfoil and the fitting with the current approach.

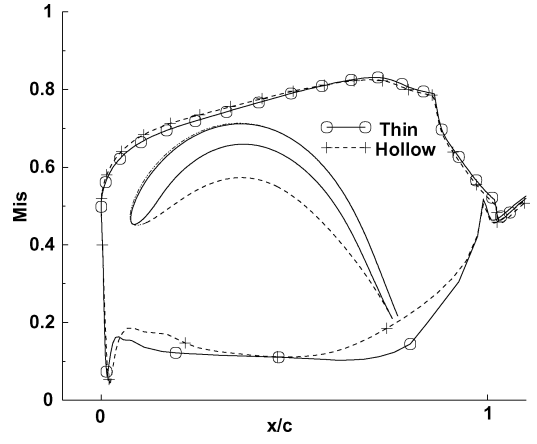

Fig. 17 Mach-number distribution of two aft-loaded airfoils with identical suction side.

Conclusions

The different alternatives to perform two-dimensional blading have been briefly reviewed. Special attention has been paid to determine the minimum degree of continuity that the surface blade should hold to have a reasonably smooth pressure distribution. The conclusion is that the resulting curve should have the slope of the curvature continuous. Theoretical, experimental and computational evidence has been given to back this idea.

We have developed a set of G^3-chained Bézier polynomials that have been conceived to design aerodynamic surfaces in the downstream direction. The position and slope of the break points is controlled by 12 blade parameters. Still it is possible to fine tune the blade by means of two additional degrees of freedom per segment. To guide the design, a graphical user interface (GUI) has been developed where the blade shape, its thickness and curvature, and the streamline that reaches the stagnation point and the isentropic Mach-number distribution obtained from an Euler code coupled with an integral boundary layer are displayed in real time. The result is a powerful, very fast, direct method to perform two-dimensional blading. During the design of this tool, the authors have been focused in the design of low-pressure-turbine blade sections; however, we have been able to reproduce with high-fidelity high-pressure-turbine airfoils with the current system as well. The design of compressors blades has not been shown to pose special problems although some customization would be convenient in a productionized version.

We have provided evidence that traditional pointwise approaches can be substituted by parametric methods to generate final geometry for turbomachinery airfoils because they are capable to reproduce the existing airfoils. We have carefully traced and numerically checked the aerodynamic behavior of several tens of existing airfoils. In all of the cases, the Mach-number distributions of the existing and the redesigned airfoils are essentially identical while the computed losses are systematically lower because of the higher degree of differentiability of the airfoil.

Acknowledgments

The authors wish to thank Industria de TurboPropulsores for the permission to publish this paper and for its support during this project. This work has been partially funded by ITP under Contract ITP-005/97 to the School of Aeronautics of the Universidad Politécnica de Madrid. The feedback and comments provided by the aerodynamic team as well as its courage using beta versions of the software are specially acknowledged.

References

[1]Giles, M., and Drela, M., "Two-Dimensional Transonic Aero-Dynamic Design Method," *AIAA Journal*, Vol. 25, No. 9, 1987, pp. 1199–1206.

[2]Dunham, J., "A Parametric Method of Turbine Blade Profile Design," American Society of Mechanical Engineers, Paper 74-GT-119, 1974.

[3]Korakianitis, T., "Design of Airfoils and Cascades of Airfoils," *AIAA Journal*, Vol. 27, No. 4, 1989, pp. 455–461.

[4]Korakianitis, T., and Papagiannidis, "Surface Curvature-Distribution Effects on Turbine Cascade Performance," *Journal of Turbomachinery*, Vol. 115, No. 2, 1993, pp. 334–341.

[5]Korakianitis, T., "Hierarchical Development of Three Direct-Design Methods for Two-Dimensional Axial Turbomachinery Cascades," *Journal of Turbomachinery*, Vol. 115, April 1993, pp. 314–324.

[6]Korakianitis, T., "Prescribed-Curvature-Distribution Airfoils for the Preliminary Geometric Design of Axial Turbomachinery Cascades," *Journal of Turbomachinery*, Vol. 115, April 1993, pp. 325–333.

[7]Korakianitis, T., and Pantazopoulos, G. I., "Improved Turbine-Blade Design Techniques Using 4th-Order Parametric-Spline Segments," *Computer Aided Design*, Vol. 25, No. 5, 1993, pp. 289–299.

[8]Corral, R., and Pastor, G., "A Parametric Design Tool for Cascades of Airfoils," *International Gas Turbine and Aeroengine Congress and Exhibition*, American Society of Mechanical Engineers, Paper 99-GT-73, Indianapolis, Indiana, June 1999.

[9]Benner, M. W., Sjolander, S. A., and Moustapha, S. C., "Influence of Leading Edge Geometry on Profile Losses in Turbines at Off-Design Incidence: Experimental Results and an Improved Correlation," *Journal of Turbomachinery*, Vol. 119, No. 2, 1997, pp. 193–199.

[10]Hodson, H. P., "Boundary-Layer Transition and Separation near the Leading Edge of a High Speed Turbine Blade," *Journal of Engineering for Gas Turbines and Power*, Vol. 107, Jan. 1985, pp. 127–134.

[11]Farin, G., *Curves and Surfaces for Computer Aided Geometric Design*, Academic Press, New York, April 1992.

[12]Hodson, H. P., and Dominy, R. G., "Three-Dimensional Flow in a Low-Pressure Turbine Cascade at its Design Condition," *Journal of Turbomachinery*, Vol. 109, 1987, pp. 177–185.

[13]Fransson, T. H., and Verdon, J. M., "Standard Configurations for Unsteady Flow Through Vibrating Axial-Flow Turbomachine-Cascades," KTH TR TRITA/KRV/92-009, Oct. 1992.

[14]Arts, T., and Rouvroit, M. L., "Aero-Thermal Performance of a Two Dimensional Highly Loaded Transonic Turbine Nozzle Guide Vane," *International Gas Turbine Conference and Exhibition*, American Society of Mechanical Engineers, Paper 90-GT-358, Brussels, Belgium, June 1990.